(Received 29 December 2024, Accepted 7 January 2025, Scheduled 11 February 2025)

# Multi-Motor Synchronous Control Strategy Based on Fuzzy Internal Model PID and Virtual Spindle Synchronous Control

Wei Yan[1, 2, *] and Shasha Li[1, 2]

[1] College of Mechanical and Electronic Engineering, Huanghe Jiaotong University, Jiaozuo 454950, China
[2] Henan Engineering Technology Research Center on Intelligent Manufacturing Technology and Equipment, Jiaozuo 454950, China

**ABSTRACT:** To achieve high-precision synchronous control of multiple motors, this study utilizes a permanent magnet synchronous motor as a case study. It adopts a fuzzy internal model proportional-integral-derivative algorithm with integral separation for single-motor control. On this basis, the virtual spindle synchronization strategy of multi-motor synchronous control and fuzzy control algorithm are further introduced to adjust the feedback torque compensation coefficient dynamically, optimizing the virtual spindle synchronization strategy. The results showed that in single-motor control, the dual closed-loop fuzzy proportional-integral control algorithm achieved a torque fluctuation error of 4 N · m when the load torque changed significantly. The fuzzy internal model proportional-integral-derivative control algorithm with integral separation had a relatively smooth adjustment process, and the maximum torque fluctuation did not exceed 1 N · m. In multi-motor synchronous control, the improved virtual spindle synchronous control strategy had a synchronization error of only 14.2 r/min between motor 1 and motor 2, as well as between motor 1 and motor 3. The single-motor and multi-motor synchronous control strategies used in the study have high control accuracy and response efficiency, which is conducive to improving the synchronization accuracy and coordination between motors. The improved strategy provides a reliable control scheme for industrial automation systems.

## 1. INTRODUCTION

With the widespread application of multi-motor drive systems in industrial automation, robotics, and other fields, the Synchronous Control (SC) problem among multiple motors has become an important research direction [1, 2]. The purpose of SC strategy is to ensure the coordinated operation of multiple motors, so that the control system has low synchronization error and high response speed, while also having strong anti-interference performance. SC strategy can be categorized into electrical synchronization and mechanical synchronization [3]. The main and secondary shafts of mechanical synchronization are connected by a series of mechanical transmission devices, and the motion state of the main shaft can be transmitted to the driven shaft through this device. If the motion state of the driven shaft changes, the main shaft will also change accordingly, ensuring synchronous operation of both. This method has a simple structure, but it has significant spatial limitations and high requirements for connection devices, making it difficult to ensure controllable accuracy [4]. In recent years, electrical synchronization has been widely used in multi-motor SC. This method does not have a mechanical transmission device but uses an upper computer to send control instructions [5]. Compared with mechanical synchronization, electrical synchronization has higher flexibility and control performance and has been widely used. However, traditional electric SC methods have poor adaptability to load changes, motor parameter fluctuations, and external disturbances in the system, which can easily lead to increased synchronization errors. Therefore, how to raise the precision, robustness, and resistance to interference of electric SC systems remains an important challenge in current research on multi-motor SC.

The control problem of synchronous motors has become a key challenge in engineering applications. Li et al. proposed a finite control set model predictive control scheme for the control problem of Permanent Magnet Synchronous Motor (PMSM). The advantages and disadvantages of this method were highlighted, and a weight factor adjustment and delay compensation scheme were adopted to improve the control method. The outcomes showed that the control capability of the reformed finite control set model predictive control scheme was greatly improved [6]. Dianov et al. proposed an improved maximum torque per ampere control algorithm to address the issues of load and motor parameter variations in synchronous motor torque maximization control. The results indicated that the algorithm could validly raise control efficiency and accuracy in practical applications, and different maximum torque per ampere control methods were applicable to different application scenarios [7]. To achieve effective control of multi-motors in high power, Rubino et al. proposed a segmented approach for vector control for multiple three-phase PMSMs. This scheme used modular modeling methods to independently control the torque of each three-phase unit and implemented a torque-sharing strategy. The results indicated that this approach could validly improve the fault tolerance and overall performance of the system, and shorten the design cycle [8]. To deal with the matter of insufficient integral control in the standard

* Corresponding author: Wei Yan (2019080910@zjtu.edu.cn).

model, Favato et al. raised a velocity form model predictive control method that combined disturbance observers. This approach was designed to eliminate bias errors in reference tracking by introducing incremental formulas. It was applied in current control driven by synchronous motors. The results indicated that this approach could validly handle unmodeled interference and parameter mismatch while providing good reference tracking performance [9].

In response to the limitations of traditional control methods, researchers from various fields have proposed various self-tuning control schemes based on fuzzy rules. Nath et al. found that the fixed value of $\lambda$ in traditional Internal Model Controller (IMC) had certain limitations. Therefore, they proposed a self-tuning scheme for the internal model Proportional-Integral-Derivative (PID) controller based on fuzzy rules. This method dynamically adjusted the value of $\lambda$ through fuzzy control rules to meet different process response requirements. The results indicated that the raised scheme had significant dynamic capability in temperature and liquid level control circuits, effectively avoiding oscillation and excessive deviation from the set values [10]. Li et al. and Adeniran et al. raised a simplified fuzzy PID controller grounded on decomposed fuzzy system design to address the shortcomings of traditional PID controllers in longitudinal dynamics control of autonomous vehicles. This method optimized and adjusted PID parameters by introducing a decomposed fuzzy system. The results indicated that the improved controller could validly optimize transient response and enhance system performance compared to traditional PID and fuzzy PID [11, 12]. To solve the problem of external disturbances in industrial temperature control systems, Liu et al. proposed a vague fractional degree PID control methodology. This algorithm used fractional order fuzzy rules to update the controller gain coefficient online. The simulation results indicated that the controller could effectively raise the operational responsiveness of the temperature control system and optimize the robustness of the system [13]. Baz et al. proposed a hybrid fuzzy PID controller for regulating the speed of electrical vans to address the dynamic modeling problem of complex vehicles. The results indicated that the proposed controller could provide smoother velocity regulation during both speeding up and slowing down phases, and maintain good control performance even in complex road conditions [14].

In summary, various motor control methods have been proposed in industry research. However, most methods cannot balance control accuracy and efficiency and are easily affected by external disturbances, resulting in low robustness. For this type of problem, taking PMSM as an example, a fuzzy internal model PID algorithm with integral separation is adopted for single-motor control, and a virtual spindle synchronization strategy is introduced to optimize multi-motor SC. Concurrently, the compensation coefficient of feedback torque undergoes dynamic adjustment through the integration of the fuzzy control algorithm, thereby enhancing the synchronization accuracy, efficiency, and robustness of multi-motor systems. The novelty of this research consists of introducing fuzzy PID control and integral separation mechanism in traditional IMC algorithms, which contributes to raising the accuracy and response speed of single-motor control, while effectively suppressing system overshoot and oscillation. Secondly, the introduction of a virtual spindle synchronization strategy optimizes multi-motor SC and solves the synchronization error problem in multi-motor systems.

## 2. METHODS AND MATERIALS

To explore high-precision multi-motor SC strategies, the study first analyzes the control strategy of a single-motor, taking PMSM as an example, and introduces the fuzzy internal model PID algorithm with integral separation. On this basis, the study further introduces a virtual spindle synchronization strategy for SC of multiple motors and dynamically adjusts the compensation coefficient of feedback torque by introducing fuzzy control algorithm to optimize the virtual spindle synchronization strategy.

### 2.1. Single-Motor Control Based on Fuzzy Internal Model PID

Single-motor systems have excellent speed regulation performance, which is a prerequisite for the stable operation of multi-motor SC systems [15]. When a multi-motor SC system encounters external disturbances, in addition to its anti-interference performance, the regulating ability of a single-motor also plays a crucial role. Therefore, before studying multi-motor SC methods, it is necessary to explore control algorithms for single-motors. The motor used in the study is PMSM. The motor consists of a rotor and a stator. During the operation of the motor, the stator is connected to three-phase AC power and generates a magnetic field in rotation. This magnetic field engages with the magnetic field produced by the permanent magnet, thereby driving the rotor to rotate. The traditional PID control algorithm has low anti-interference performance and poor control effect for PMSM control [16]. To this end, the study introduces the IMC algorithm and combines it with the PID algorithm to form the internal model PID algorithm, which is used to adjust the three major parameters of proportional, integral, and derivative ones in the PID algorithm. The IMC algorithm is predicated on a relatively simple design principle that exhibits high efficiency. This design principle enables real-time parameter adjustment, thereby enhancing the control effect. The diagrammatic representation of the IMC structure is shown in Figure 1.

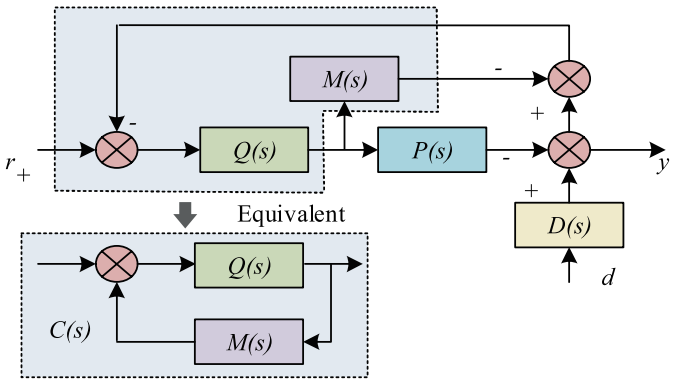


**FIGURE 1**. IMC structure diagram.

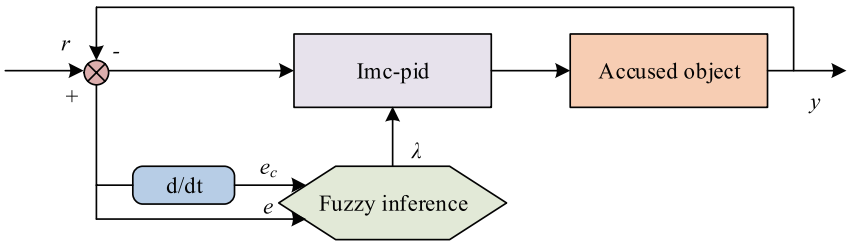


**FIGURE 2**. The framework of the fuzzy internal model PID algorithm.

In Figure 1, $r$ and $y$ respectively represent input and output signals. $d$ represents external interference signals, $Q(s)$ the IMC, $P(s)$ the subject of control, and $M(s)$ the math-model of $P(s)$. To ease the process of calculating the transfer function between input and output, the original structure is equivalently treated, and a feedback controller is introduced. Its calculation is shown in Equation (1) [17].

$$C(s) = \frac{Q(s)}{1 - Q(s)M(s)} \tag{1}$$

In Equation (1), $C(s)$ represents the feedback controller of the equivalent diagram of the internal model structure. When $r$ and $y$ are used as inputs and outputs, their transfer functions are shown in Equation (2).

$$\frac{y}{r} = \frac{C(s)P(s)}{1 + C(s)P(s)} \tag{2}$$

When $d$ and $y$ are used as inputs and outputs, their transfer functions are shown in Equation (3).

$$\frac{y}{d} = \frac{D(s)}{1 + C(s)P(s)} \tag{3}$$

Substituting Equation (1) into Equations (2) and (3) yields Equation (4).

$$\begin{cases} \dfrac{y}{r} = \dfrac{Q(s)P(s)}{1 + Q(s)[P(s) - M(s)]} \\ \dfrac{y}{d} = \dfrac{[1 - Q(s)M(s)]D(s)}{1 + Q(s)[P(s) - M(s)]} \end{cases} \tag{4}$$

When the inputs are $r$ and $d$, the transfer function expression is show in Equation (5).

$$y = \frac{Q(s)P(s)}{1+Q(s)[P(s)-M(s)]}r + \frac{[1-Q(s)M(s)]D(s)}{1+Q(s)[P(s)-M(s)]}d \tag{5}$$

When $P(s)$ is in a stable state, $M(s) = P(s)$ is obtained. If there is an inverse of $M(s)$, the designed IMC needs to be equal to the inverse of $M(s)$, so that the input and output remain consistent. Therefore, an ideal controller system is not affected by input and interference, and can achieve error free tracking output in any situation. However, there is a lag link in $M(s)$, and the controller designed based on the inverse of $M(s)$ does not satisfy the causal law. Therefore, in the design of the IMC, the research mainly splits the design of the IMC and then carries out corresponding design. The specific design steps are to first decompose $M(s)$ into $M_+(s)$ and $M_-(s)$, where $M_+(s)$ has a pure hysteresis component, and $M_-(s)$ is the minimum phase component. Then, a filter is added to the inverse of $M_-(s)$, as shown in Equation (6).

$$Q(s) = \frac{f(s)}{M_-(s)} \tag{6}$$

In Equation (6), $\alpha$ represents a filter that passes low frequencies, and its calculation is shown in Equation (7).

$$f(s) = \frac{1}{(1 + \alpha s)^\eta} \tag{7}$$

In Equation (7), $\alpha$ represents the time constant, which can regulate the system's operational efficiency. $\alpha$ mainly affects the dynamic response of controller $Q(s)$ by controlling the "cut-off frequency" of the filter. When $\alpha$ is smaller, the filter attenuates low-frequency signals less, and the system can respond to input signals more quickly. On the contrary, increasing $\alpha$ will reduce the system's response to high-frequency signals, making the system less sensitive to noise and high-frequency components. $\eta$ is a parameter that ensures the feasibility of the IMC. However, the internal model PID algorithm is difficult to balance the stable performance of the motor during start-up and disturbance [18]. For this purpose, fuzzy control is further introduced in the study, and the control parameter $\lambda$ is proposed to modify the PID parameters in immediate time. The schematic diagram of the framework of the fuzzy internal model PID algorithm is shown in Figure 2.

In Figure 2, the input of the fuzzy internal model PID control system includes error e and error change rate $e_c$. The variable $\lambda$ is derived by fuzzy inference, and the three major parameters of the internal model PID are adjusted accordingly. Subsequently, it acts on the controlled object to achieve effective control. When the deviation is large, the value of $\lambda$ is large; otherwise it is small. Fuzzy algorithm can adjust the three parameters of internal model PID by adjusting the value of $\lambda$, but this process may lead to overshoot. The reason is that when the motor is just started, the integral will begin to accumulate deviation, causing overshoot [19, 20]. To avoid this phenomenon, the study further introduces the idea of integral separation. The simulation model of the fuzzy internal model PID controller incorporating the idea of integral separation is shown in Figure 3.

As shown in Figure 3, Wm1 represents the input signal of the integrator, and 30/pi is the scaling factor. After adjusting

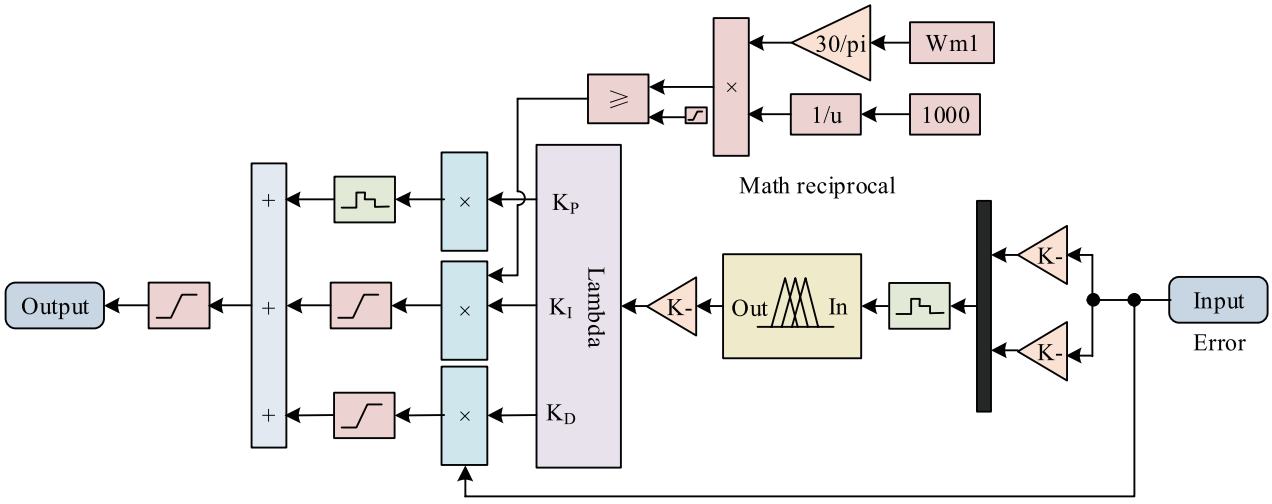


**FIGURE 3**. Fuzzy internal model PID controller introducing integral separation concept.

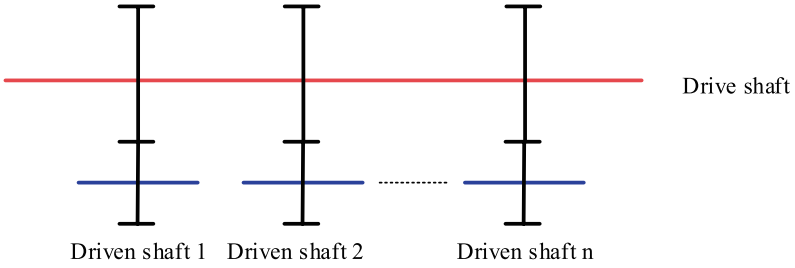


**FIGURE 4**. Structural diagram of mechanical spindle SC.

the proportional factor of the input signal, it enters the integrator, which calculates the accumulated total of the input signal and outputs the integration result. The core idea of integral separation is that the integral effect does not always exist in the control process, but is dynamically added or separated according to actual needs. Specifically, during the response start-up phase of the system, the integration process is gradually introduced when the system output approaches the set target value to eliminate static errors in the system. The fuzzy internal model PID control algorithm with integral separation is a system that primarily controls the activation of integral action by establishing triggering conditions. This ensures that excessive accumulation of integral terms is avoided in the early stage of startup, thereby preventing overshoot. Additionally, integral action is employed to eliminate steady-state errors when the system gradually approaches a steady state. This method effectively improves the corresponding speed and enhances the stability of the system through fuzzy control and dynamic PID parameter adjustment.

### 2.2. Multi-Motor Virtual Spindle SC Strategy

By designing a single-motor control method based on fuzzy internal model PID controller, the dynamic performance of the control system is enhanced. On this basis, further analysis is conducted on the multi-motor SC strategy. The traditional mechanical synchronization strategy is prone to mechanical damage and lacks flexibility. Therefore, the study introduces a virtual spindle synchronization strategy. This strategy is developed for SC of mechanical spindles, and the specific structural diagram is shown in Figure 4.

In Figure 4, the master and slave axes are mechanically connected, with the main axis driven by a motor and the slave axis moving through the mechanical connection. At the same time, the motion feedback from the axis will be transmitted to the main axis, and the two will be coupled with each other. Unlike traditional mechanical spindle SC, virtual spindle belongs to the electric SC strategy, which mainly sets up a virtual spindle to transmit input signals from the shaft. At the same time, a feedback loop is set up to ensure that the rotational speed of the spindle and the slave shaft remains coupled. In addition, the virtual spindle synchronization strategy mainly achieves SC by changing the spindle parameters. The schematic diagram of virtual spindle SC with three motors is shown in Figure 5.

In Figure 5, $J_m$ means the inertia of the spindle's rotational mass, $T_i$ the torque transmitted to the spindle by each driven axis, $T$ the driving torque received by the spindle, $\omega*$ the input angular velocity, $\omega_m$ the angular velocity of the virtual spindle, and $\omega_1$, $\omega_2$, and $\omega_3$ represent the angular velocities of each slave axis. Similar to the real spindle, the virtual spindle will be driven to move from the spindle by a driving torque. The expression for the relationship between the angular velocity and torque of the spindle is shown in Equation (8).

$$T - \sum T_i = J_m \frac{d\omega_m}{dt} \tag{8}$$

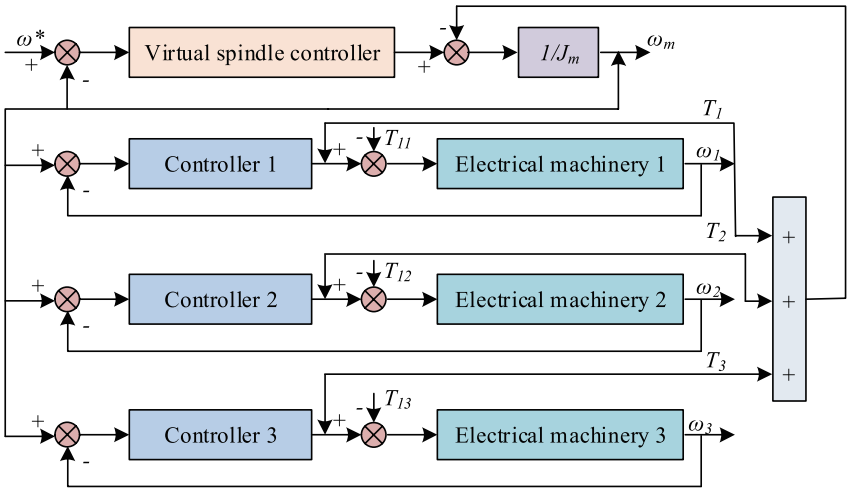


**FIGURE 5**. Schematic diagram of virtual spindle SC with three motors.

In Equation (8), $dt$ represents the derivative of time, and the calculation of $T$ is shown in Equation (9).

$$T = B_m(\omega^* - \omega_m) + K_m \int(\omega^* - \omega_m)dt \quad (9)$$

In Equation (9), $B_m$ represents the attenuation coefficient of the spindle. $\omega^*$ represents angular velocity, which needs to be set in advance. $K_m$ represents the elasticity coefficient of the spindle. The calculation of $T_i$ is similar to that of $T$. Considering the mechanical connection device between the master and slave shafts, which is easily affected by damping and elasticity, the calculation of $T_i$ can be obtained as shown in Equation (10).

$$T_i = B_i(\omega_m - \omega_i) + K_i \int(\omega_m - \omega_i)dt \quad (10)$$

In Equation (10), $\omega_m$ represents the attenuation coefficient of the driven shaft. $\omega_i$ means the actual rotational speed of the driven shaft. $K_i$ means the elastic coefficient of the driven shaft. In the three motor SC model, the virtual spindle will provide inputs for all motors. Under the ideal SC, the synchronization error remains zero when all motors are operating. At this point, the angular acceleration of the virtual spindle is zero; the system is stable; and the motor speed is synchronized. However, when a certain motor is subjected to external disturbances, its speed will rapidly decrease, causing errors in the speed of that motor compared to other motors. To restore synchronization, the system needs to increase feedback torque to adjust the speed of the disturbance motor. The traditional virtual spindle synchronization control method can achieve motor synchronization control to a certain extent. However, when a specific motor is disturbed, merely increasing the feedback torque can lead to an accelerated decrease in spindle speed, thereby compromising the synchronization accuracy and system stability of other motors [21]. Therefore, an improved virtual spindle SC method is proposed, which rewrites the feedback torque from the axis to the spindle, as shown in Equation (11).

$$T_i = B_i(\omega_m - \omega_i) + K_i \int(\omega_m - \omega_i)dt + k \cdot c \cdot (\omega'') \quad (11)$$

In Equation (11), $c$ represents the conditional coefficient, and $k$ represents the compensation coefficient. Unlike the original feedback mechanism, the improved feedback mechanism adds $k \cdot c \cdot (\omega''$, which takes a value of 0 when not being disturbed, and not 0 when being disturbed. This approach is beneficial for rapidly reducing synchronization errors and improving the efficiency and accuracy of SC response. Among them, the compensation coefficient $k$ characterizes the magnitude of the feedback torque. When eliminating synchronization errors, the larger the error is, the larger the value of $k$ is. When the error is small, $k$ decreases accordingly to ensure system stability. The adjustment of the compensation coefficient $k$ is mainly carried out using fuzzy algorithms. ($\omega''$ is set as the error e of the fuzzy controller, together with the error change rate $e_c$ as the input and $k$ as the output. The fuzzy rule set is presented in Table 1.

**TABLE 1**. Fuzzy rule table.

| E/K/$E_c$ | B | M | S | ZO |
|---|---|---|---|---|
| B | B | B | B | B |
| M | B | M | M | M |
| S | M | M | S | S |
| N | M | M | S | ZO |
| ZO | M | S | S | ZO |

In Table 1, K is the language variable of $k$. E and $E_c$ are the linguistic variables of error e and error rate of change $e_c$, respectively. In fuzzy sets, ZO represents 0; N represents negative; and B, M, and S represent large, medium, and small, respectively. E contains four variables: B, M, S, and NO, while $E_c$ contains five variables: B, M, S, NO, and N. A total of 20 fuzzy rules are obtained in Table 1, expressed in the form of "if (E is B) and (Ec is N) then (K is M)". The optimized SC model that dynamically adjusts the value of $k$ using fuzzy algorithm is shown in Figure 6.

## 3. RESULTS

The study first verified the effectiveness of the fuzzy internal model PID control algorithm with integral separation in single-

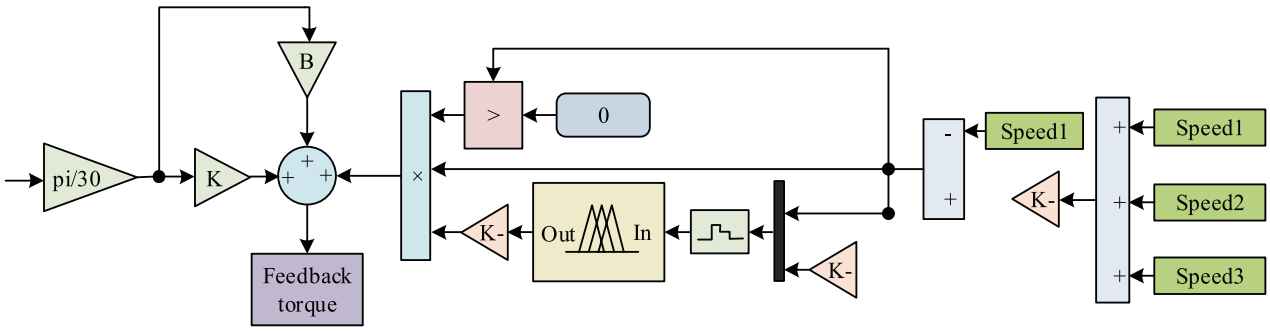


**FIGURE 6**. Improved SC model.

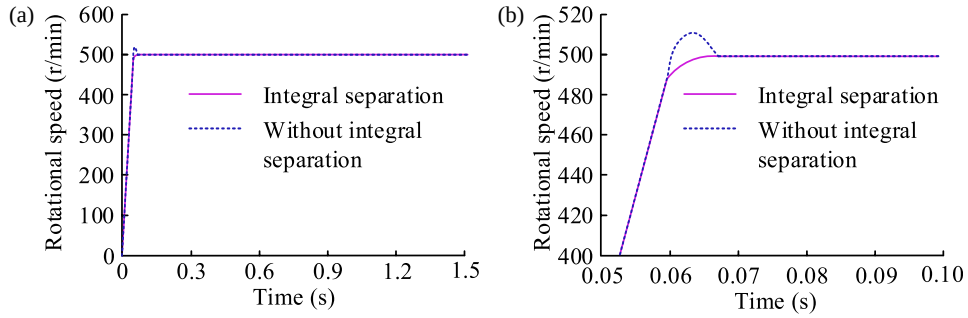


**FIGURE 7**. The speed variation of various control algorithms. (a) Speed variation curve. (b) Partial enlarged image.

motor control and compared it with the dual closed-loop fuzzy (CLF) PI control algorithm. On this basis, the effectiveness of the improved virtual spindle SC strategy for multi-motor SC was verified, and the master-slave SC method, deviation coupling control method, and unimproved virtual spindle SC method were selected for comparison.

### 3.1. Simulation Analysis of Single-Motor Control Strategy

To confirm the validity of the single-motor control algorithm based on fuzzy internal model PID control algorithm, a PMSM speed control system simulation model was constructed in Simulink simulation environment using PMSM as an example. The motor parameters in the model are shown in Table 2.

**TABLE 2**. Motor parameters.

| Name | Numeric value |
|---|---|
| Number of electrodes | 4 |
| Stator resistance | 0.958 Ω |
| Stator inductance | 12 mH |
| Flux linkage | 0.1827 Wb |
| Damping coefficient | 0.008 N · m · s |
| Moment of inertia | 0.003 kg · $m^2$ |

The study first verified the speed variation of the fuzzy internal model PID control algorithm with integral detachment and the fuzzy internal model PID control method without integral separation under the same simulation conditions. The target speed was set to 500 r/min; the simulation duration was 0.15 s; and the load torque (LT) was increased to 15 N · m at 0.5 s. Under these conditions, the speed changes of the two control methods are shown in Figure 7. From Figure 7, during the motor start-up phase, the fuzzy internal model PID control algorithm with integral separation could effectively suppress overshoot and improve the system's stability.

To confirm the effectiveness of the fuzzy internal model PID control method with integral detachment, double CLF PI control algorithm was further compared with it. The simulation duration was set to 0.4 seconds. At $t = 0$ s, the LT applied to the motor was 0 N · m. At 0.2 s, the LT was increased to 40 N · m and the speed raised to 100 r/min. The torque was reduced to 20 N · m at 0.3 s and the speed increased to 200 r/min. The simulation results of the dual CLF PI control method are in Figure 8. From Figure 8, the dual CLF PI control algorithm exhibited good dynamic characteristics in reaction to variations in velocity and torque. The system could quickly respond to changes in speed and torque and achieve a relatively fast adjustment process. As shown in Figure 8(a), the system could adjust the output within 0.02 seconds when the set speed changed, ensuring precise control of the system. However, there was a certain overshoot phenomenon in the system throughout the process of adjusting speed. When the system attempted to reach the target speed, the speed would quickly increase to 220 r/min and then gradually fall back to a stable state, which led to insufficient smoothness in speed control and affected the system's regulation effect. In Figure 8(b), when the LT changes significantly, there was a large pulsation phenomenon in the torque output, and the fluctuation error reached 4 N · m, resulting in the instability of the motor output.

The simulation results of the fuzzy internal model PID control method with integral detachment are in Figure 9. From Figure 9(a), in the fuzzy internal model PID control method with integral detachment, the response time of the speed was

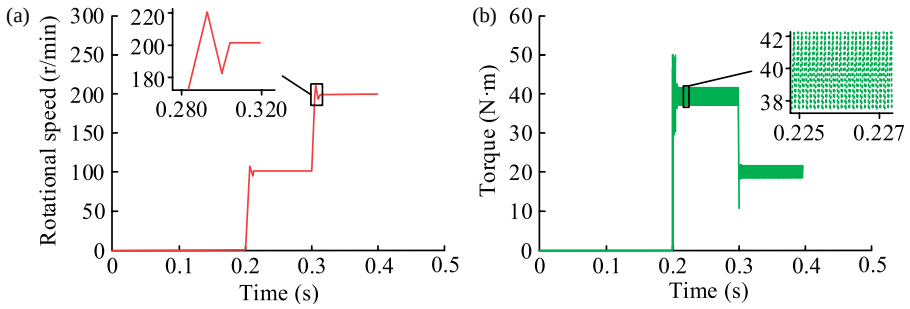


**FIGURE 8**. Speed and torque output of dual CLF PI control algorithm. (a) Speed variation curve. (b) Torque variation curve.

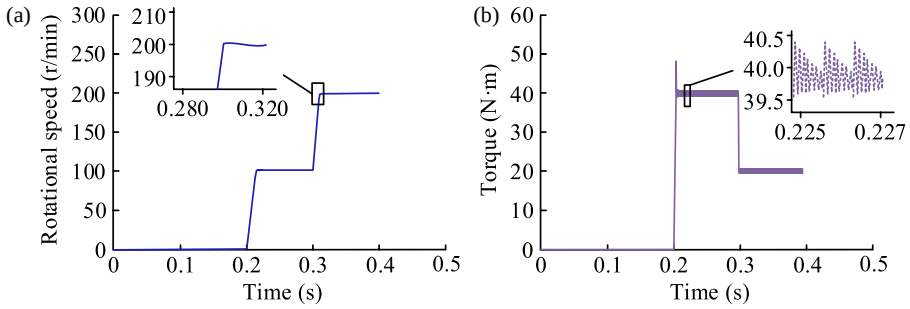


**FIGURE 9**. Speed and torque output of fuzzy internal model PID control algorithm. (a) Speed variation curve. (b) Torque variation curve.

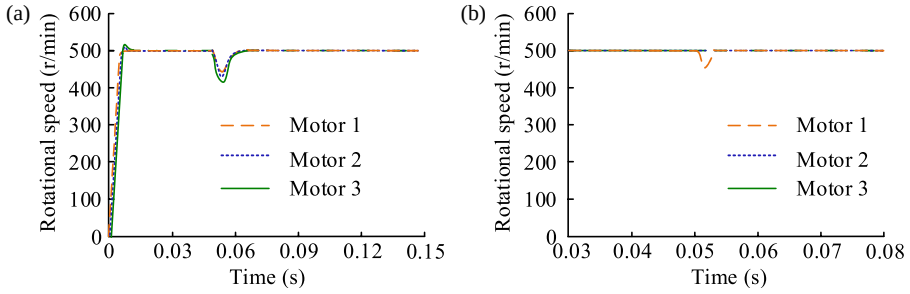


**FIGURE 10**. Changes in motor speed in master-slave SC strategy. (a) Motor 1 applies load. (b) Motor 3 applies load.

only 0.03 s when the load changed. Meanwhile, the fuzzy internal model PID control method with integral detachment could effectively suppress speed overshoot and avoid overshoot phenomenon. As shown in Figure 9(b), when there was an abrupt shift in LT, the fuzzy internal model PID control method with integral detachment could respond in a timely manner, and the adjustment process was relatively smooth. Among them, the maximum torque fluctuation did not exceed 1 N · m, which effectively reduced torque fluctuation and alleviated overshoot compared to the dual closed-loop control algorithm.

### 3.2. Simulation Analysis of Multi-Motor SC Strategy

To verify the effectiveness of the improved virtual spindle SC strategy for multi-motor SC, a fuzzy internal model PID control algorithm was adopted as the single-motor control method, and a three motor simulation model was built in Simulink environment. The reference speed was scheduled to 500 r/min and the simulation time scheduled to 0.15. Meanwhile, the study compared the master-slave SC method, deviation coupling control method, and unimproved virtual spindle SC method with the proposed control strategy. Two simulations were conducted in the master-slave SC method. At 0.05 s for the first time, the LT carried by the first motor was raised from 0 N · m to 15 N · m. The second simulation was to increase the LT of the third motor from 0 N · m to 15 N · m at 0.05 s. The speed changes of each motor in the two simulations are shown in Figure 10. As shown in Figure 10(a), when a load was applied to motor 1 at 0.05 s, there was a certain lag in all other motors. As shown in Figure 10(b), when an LT was applied to motor 3, the other motors were not affected. The reason is that in this control strategy, the speed is unidirectionally coupled and can only be influenced by the main shaft and the secondary shaft, which cannot affect the main shaft.

The research continued to simulate and compare the deviation coupling control method, unimproved virtual spindle SC method, and raised control methodology. In the simulation setting, the LT of the first motor was increased from 0 N · m to 15 N · m at 0.05 s. The speed changes of each control strategy are shown in Figure 11. In Figure 11(a), in the deviation coupling control method, when a load was applied to motor 1, motor 1 compensated for the coupled motor 3, resulting in a significant decrease in the speed of motor 3. Subsequently, the

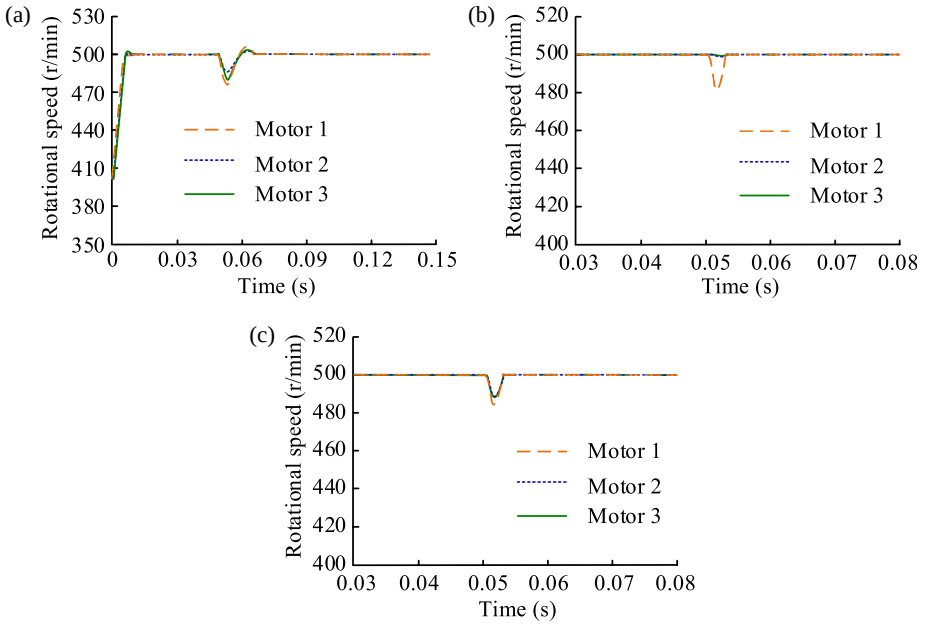


**FIGURE 11**. Changes in rotational speed of various control strategies. (a) Deviation coupling control method. (b) Unimproved virtual spindle synchronization control method. (c) Improved virtual spindle synchronization control method.

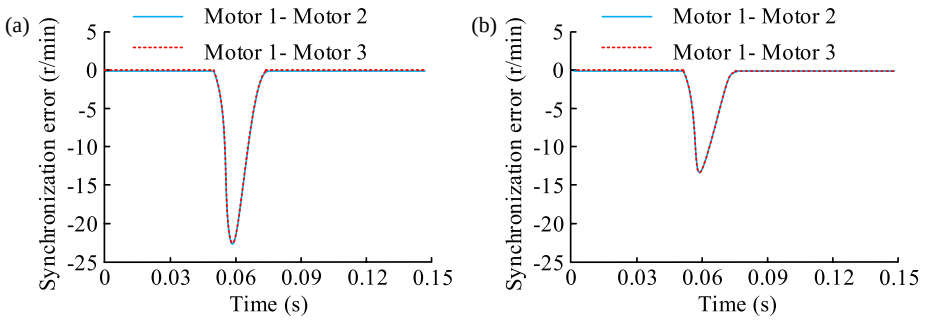


**FIGURE 12**. Synchronization error of each motor in different control strategies. (a) Error of virtual spindle synchronization control strategy before improvement. (b) Error of virtual spindle synchronization control strategy after improvement.

speed of motor 2 decreased. Therefore, the descent amplitude of motor 3 was greater than that of motor 2. As shown in Figure 11(b), in the unimproved virtual spindle SC method, when a load was applied to motor 1, its speed rapidly decreased, driving the other motors to decrease together, but the decrease was not significant. From Figure 11(c), the improved virtual spindle SC method had a greater response to load changes and would drive the speed of other motors to rapidly decrease following motor 1, reducing the synchronization error between each motor. Overall, the improved virtual spindle SC method had better SC effect.

Further research was conducted to verify the synchronization errors of each motor in the virtual spindle SC strategy before and after improvement, as shown in Figure 12. In Figure 12(a), in the unimproved virtual spindle SC strategy, the synchronization error between motor 1 and motor 2, as well as motor 1 and motor 3 was as high as 24.6 r/min. According to Figure 12(b), in the improved virtual spindle SC strategy, the synchronization error between motor 1 and motor 2, as well as motor 1 and motor 3 was only 14.2 r/min, which was significantly better than the original control strategy.

## 4. DISCUSSION AND CONCLUSION

To achieve high-precision and high-efficiency multi-synchronous motor control, a fuzzy internal model PID control algorithm with integral detachment and an improved virtual spindle SC strategy were proposed. The results showed that in single-motor control, compared with the fuzzy internal model PID control algorithm without integral separation, the control algorithm with integral separation could effectively suppress system overshoot. The double CLF PI control system had a large overshoot when being disturbed. The improved fuzzy internal model PID control algorithm could effectively avoid this phenomenon. The reason is that the integral separation mechanism can adjust the integral action promptly when the system is disturbed, avoiding the overshoot phenomenon caused by excessive integral action. In multi-motor SC, the master-slave SC strategy suffered from time delay and overshoot accumulation. In the deviation coupling control method, when a load was applied to motor 1, motor 1 compensated for the coupled motor 3, resulting in a significant decrease in motor 3's speed. In the unimproved virtual spindle SC method, when a load was applied to motor 1, its speed rapidly

decreased, but the synchronization error with other motors was relatively large. The improved virtual spindle SC method had a greater response to load changes and would drive the speed of other motors to rapidly decrease following motor 1, reducing the synchronization error between one motor and another motor. The single-motor and multi-motor SC strategies had significant advantages, ensuring control accuracy while also quickly responding to load changes. There are still two potential research directions for the study. Firstly, in the virtual spindle synchronization control strategy, the various parameters of the virtual spindle can be flexibly adjusted to achieve better control performance of the synchronization system. However, the research used the empirical trial and error method when adjusting parameters, which has insufficient accuracy. Future research can explore the application of heuristic optimization algorithms to parameter optimization to achieve higher precision SC. Secondly, the analysis was mainly conducted in the Simulink simulation environment. Although the control platform was built, experiments have not yet been carried out. Subsequent research needs to explore the control effectiveness of the proposed multi-motor SC strategy in practical applications.

## ACKNOWLEDGEMENT

This study was supported by General Science Foundation Project "Research on Chaos Identification Mechanism of Vibration Cutting Based on Dynamic Fracture Theory" (242300420038).

## REFERENCES

[1] Fang, P., Y. Wang, M. Zou, and Z. Zhang, "Combined control strategy for synchronization control in multi-motor-pendulum vibration system," *Journal of Vibration and Control*, Vol. 28, No. 17-18, 2254–2267, 2022.

[2] Shi, G., P. Qiao, D. Sang, S. Wang, and M. Song, "Synchronous and fault-tolerance control for dual-motor steer-by-wire system of commercial vehicle," *Proceedings of the Institution of Mechanical Engineers, Part D: Journal of Automobile Engineering*, Vol. 238, No. 7, 1964–1980, 2024.

[3] Giang, P. T., V. T. Ha, and V. H. Phuong, "Drive control of a permanent magnet synchronous motor fed by a multi-level inverter for electric vehicle application," *Engineering, Technology & Applied Science Research*, Vol. 12, No. 3, 8658–8666, 2022.

[4] Wei, Y., M. Qiao, and P. Zhu, "Fault-tolerant operation of five-phase permanent magnet synchronous motor with independent phase driving control," *CES Transactions on Electrical Machines and Systems*, Vol. 6, No. 1, 105–110, 2022.

[5] Shi, P., W. Sun, X. Yang, I. J. Rudas, and H. Gao, "Master-slave synchronous control of dual-drive gantry stage with cogging force compensation," *IEEE Transactions on Systems, Man, and Cybernetics: Systems*, Vol. 53, No. 1, 216–225, 2022.

[6] Li, T., X. Sun, G. Lei, Y. Guo, Z. Yang, and J. Zhu, "Finite-control-set model predictive control of permanent magnet synchronous motor drive systems — An overview," *IEEE/CAA Journal of Automatica Sinica*, Vol. 9, No. 12, 2087–2105, 2022.

[7] Dianov, A., F. Tinazzi, S. Calligaro, and S. Bolognani, "Review and classification of MTPA control algorithms for synchronous motors," *IEEE Transactions on Power Electronics*, Vol. 37, No. 4, 3990–4007, 2021.

[8] Rubino, S., O. Dordevic, R. Bojoi, and E. Levi, "Modular vector control of multi-three-phase permanent magnet synchronous motors," *IEEE Transactions on Industrial Electronics*, Vol. 68, No. 10, 9136–9147, 2020.

[9] Favato, A., P. G. Carlet, F. Toso, R. Torchio, and S. Bolognani, "Integral model predictive current control for synchronous motor drives," *IEEE Transactions on Power Electronics*, Vol. 36, No. 11, 13 293–13 303, 2021.

[10] Nath, U. M., C. Dey, and R. K. Mudi, "Fuzzy rule-based autotuned internal model controller for real-time experimentation on temperature and level processes," *International Journal of Automation and Control*, Vol. 14, No. 2, 239–256, 2020.

[11] Li, R., S. Deng, and Y. Hu, "Autonomous vehicle modeling and velocity control based on decomposed fuzzy PID," *International Journal of Fuzzy Systems*, Vol. 24, No. 5, 2354–2362, 2022.

[12] Adeniran, A. O., O. Olabisi, A. O. Akankpo, *et al.*, "Modelling and comparative analysis of inductively coupled circular and square loop wireless power transfer at UHF band for automobile charging," *Acta Electronica Malaysia*, Vol. 7, No. 1, 08–14, 2023.

[13] Liu, L., D. Xue, and S. Zhang, "General type industrial temperature system control based on fuzzy fractional-order PID controller," *Complex & Intelligent Systems*, Vol. 9, No. 3, 2585–2597, 2023.

[14] Baz, R., K. E. Majdoub, F. Giri, and A. Taouni, "Self-tuning fuzzy PID speed controller for quarter electric vehicle driven by In-wheel BLDC motor and Pacejka's tire model," *IFAC-PapersOnLine*, Vol. 55, No. 12, 598–603, 2022.

[15] Mehedi, F., H. Benbouhenni, L. Nezli, and D. Boudana, "Feed-forward neural network-DTC of multi-phase permanent magnet synchronous motor using five-phase neural space vector pulse width modulation strategy," *Journal Européen des Systèmes Automatisés*, Vol. 54, No. 2, 345–354, 2021.

[16] Xu, K., W. Liang, W. Zhao, C. Wang, S. Zou, and X. Zhou, "Vehicle stability and synchronization control of dual-motor steer-by-wire system considering multiple uncertainties," *IEEE Transactions on Transportation Electrification*, Vol. 10, No. 2, 3092–3104, 2023.

[17] Luo, N., H. Yu, Z. You, Y. Li, T. Zhou, Y. Jiao, N. Han, C. Liu, Z. Jiang, and S. Qiao, "Fuzzy logic and neural network-based risk assessment model for import and export enterprises: A review," *Journal of Data Science and Intelligent Systems*, Vol. 1, No. 1, 2–11, 2023.

[18] Ding, H., Y. Liu, and Y. Zhao, "A new hydraulic synchronous scheme in open-loop control: Load-sensing synchronous control," *Measurement and Control*, Vol. 53, No. 1-2, 119–125, 2020.

[19] Veerendar, T., D. Kumar, and V. Sreeram, "Fractional-order PID and internal model control-based dual-loop load frequency control using teaching-learning optimization," *Asian Journal of Control*, Vol. 25, No. 4, 2482–2497, 2023.

[20] Ti, Y., R. Wang, T. Song, and W. Zhao, "The study of a unified driver model controller based on fractional-order PIλDμ and internal model control," *Proceedings of the Institution of Mechanical Engineers, Part D: Journal of Automobile Engineering*, Vol. 237, No. 9, 2374–2383, 2023.

[21] Chu, C.-W., Z.-C. Zhu, H.-T. Bian, and J.-C. Jiang, "Design of self-heating test platform for sulfide corrosion and oxidation based on Fuzzy PID temperature control system," *Measurement and Control*, Vol. 54, No. 5-6, 1082–1096, 2021.